

Support Information

High-Efficient Photo- and Electro-catalytic Materials Based on Basket-like {Sr \subset P₆Mo₁₈O₇₃} Cage

Kai Yu^{a,b}, He Zhang^{a,b}, Jing-hua Lv^{a*}, Li-hong Gong^{a,b}, Chun-mei Wang^{a,b}, Lu Wang^c, Chun-xiao Wang^{a,b}, Bai-Bin Zhou^{a,b*}

1. Structural figures

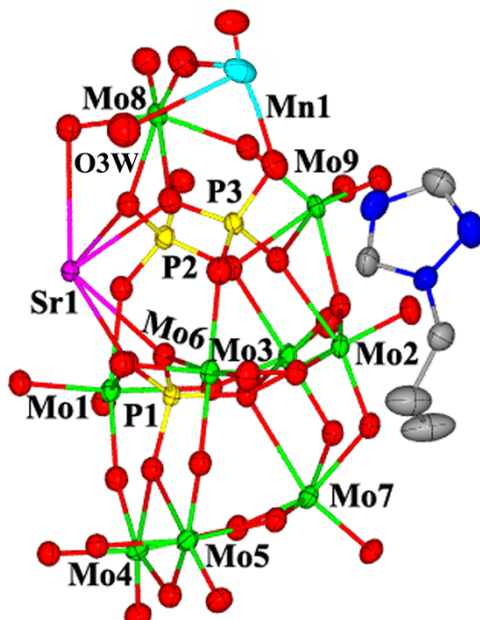


Figure S1 ORTEP view of the basic units in compound **1** with 50% thermal ellipsoid.

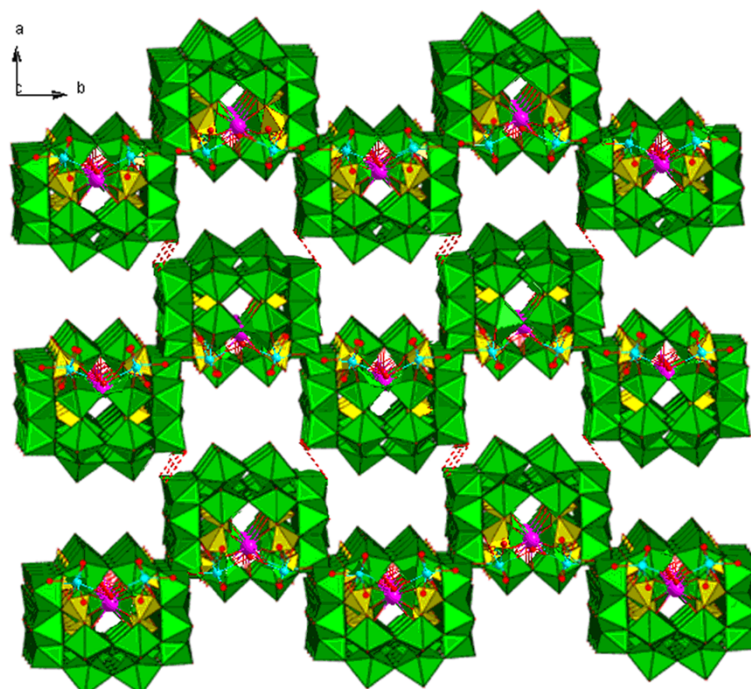


Figure S2 The 3-D supramolecular network on the ab plane of compound **1**.

2. Structural data

Table S1 Selected bond lengths (\AA) and bond angles ($^\circ$) of compound **1**

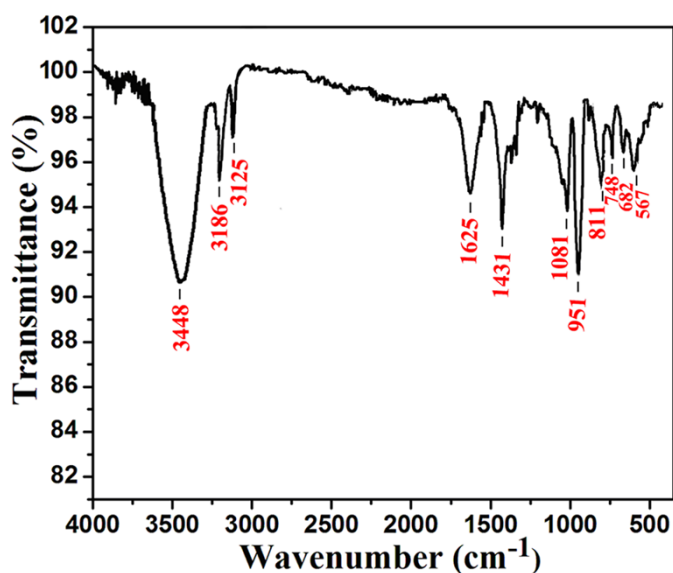
Mo(1)-O(34)	1.678(8)	Mo(1)-O(2)	1.8707(13)	Mo(1)-O(26)	2.025(7)
Mo(1)-O(16)	1.862(8)	Mo(1)-O(6)	2.224(7)	Mo(1)-O(17)	2.061(7)
Mo(2)-O(28)	1.691(8)	Mo(2)-O(18)	1.778(8)	Mo(2)-O(14)	1.800(8)
Mo(2)-O(5)	2.049(8)	Mo(2)-O(20)	2.141(7)	Mo(2)-O(23)	2.459(7)
Mo(3)-O(38)	1.676(8)	Mo(3)-O(26)	1.787(7)	Mo(3)-O(9)	1.805(7)
Mo(3)-O(5)	2.064(8)	Mo(3)-O(24)	2.150(7)	Mo(3)-O(23)	2.361(7)
Mo(4)-O(35)	1.677(8)	Mo(4)-O(13)	1.8751(11)	Mo(4)-O(16)	1.898(8)
Mo(4)-O(15)	1.985(8)	Mo(4)-O(21)	2.069(7)	Mo(4)-O(11)	2.298(7)
Mo(5)-O(36)	1.682(8)	Mo(5)-O(7)	1.877(8)	Mo(5)-O(8)	1.8801(12)
Mo(5)-O(15)	1.981(8)	Mo(5)-O(12)	2.057(7)	Mo(5)-O(11)	2.291(7)
Mo(6)-O(31)	1.679(8)	Mo(6)-O(1)	1.8617(13)	Mo(6)-O(7)	1.877(8)
Mo(6)-O(18)	2.031(7)	Mo(6)-O(19)	2.049(8)	Mo(6)-O(4)	2.238(7)
Mo(7)-O(29)	1.695(7)	Mo(7)-O(21)	1.803(8)	Mo(7)-O(12)	1.805(7)
Mo(7)-O(9)	2.059(8)	Mo(7)-O(14)	2.086(8)	Mo(7)-O(23)	2.408(7)
Mo(8)-O(32)	1.697(9)	Mo(8)-O(40)	1.696(10)	Mo(8)-O(3)	1.8913(19)
Mo(8)-O(33)	1.985(8)	Mo(8)-O(22)	2.243(8)	Mo(8)-O(27)	2.279(8)
Mo(9)-O(37)	1.709(8)	Mo(9)-O(30)	1.717(8)	Mo(9)-O(33)	1.831(8)
Mo(9)-O(5)	2.037(7)	Mo(9)-O(20)	2.296(7)	Mo(9)-O(24)	2.322(7)
P(1)-O(6)	1.517(8)	P(1)-O(11)	1.536(8)	P(2)-O(17)	1.516(8)
P(1)-O(4)	1.523(8)	P(1)-O(23)	1.573(7)	P(2)-O(22)	1.523(8)
P(2)-O(24)	1.553(8)	P(3)-O(27)	1.510(8)	P(3)-O(19)	1.536(9)
P(2)-O(10)	1.569(8)	P(3)-O(25)	1.536(9)	P(3)-O(20)	1.572(8)
Sr(1)-O(27)#1	2.557(8)	Sr(1)-O(22)#1	2.594(7)	Sr(1)-O(4)	2.653(7)
Sr(1)-O(27)	2.557(8)	Sr(1)-O(22)	2.594(7)	Sr(1)-O(4)#1	2.653(7)
Sr(1)-O(6)	2.664(7)	Sr(1)-O(6)#1	2.664(7)	Sr(1)-O(3)	2.864(11)
Mn(1)-O(39)	1.823(16)	Mn(1)-O(25)	2.045(10)	Mn(1)-O(30)#2	2.328(9)
Mn(1)-O(40)	2.379(11)	Mn(1)-O(34)#3	2.488(9)		
O(34)-Mo(1)-O(16)	101.4(4)	O(28)-Mo(2)-O(18)	104.0(4)	O(38)-Mo(3)-O(26)	104.2(4)
O(34)-Mo(1)-O(2)	99.5(4)	O(28)-Mo(2)-O(14)	103.3(4)	O(38)-Mo(3)-O(9)	103.0(4)
O(34)-Mo(1)-O(26)	93.1(3)	O(28)-Mo(2)-O(5)	99.6(4)	O(38)-Mo(3)-O(5)	96.3(4)
O(34)-Mo(1)-O(17)	95.1(3)	O(28)-Mo(2)-O(20)	97.9(3)	O(38)-Mo(3)-O(24)	95.4(3)
O(34)-Mo(1)-O(6)	172.0(3)	O(28)-Mo(2)-O(23)	170.5(3)	O(38)-Mo(3)-O(23)	169.5(3)
O(35)-Mo(4)-O(13)	101.1(4)	O(36)-Mo(5)-O(7)	101.8(4)	O(31)-Mo(6)-O(1)	98.7(4)
O(35)-Mo(4)-O(16)	101.0(4)	O(36)-Mo(5)-O(8)	99.5(4)	O(31)-Mo(6)-O(7)	101.4(4)
O(35)-Mo(4)-O(15)	100.0(4)	O(36)-Mo(5)-O(15)	98.9(4)	O(31)-Mo(6)-O(18)	94.6(3)
O(35)-Mo(4)-O(21)	94.7(3)	O(36)-Mo(5)-O(12)	95.4(3)	O(31)-Mo(6)-O(19)	95.3(4)
O(35)-Mo(4)-O(11)	170.3(3)	O(36)-Mo(5)-O(11)	170.0(3)	O(31)-Mo(6)-O(4)	173.3(4)
O(29)-Mo(7)-O(21)	105.6(4)	O(32)-Mo(8)-O(40)	101.9(5)	O(37)-Mo(9)-O(30)	102.5(4)
O(29)-Mo(7)-O(12)	105.8(4)	O(32)-Mo(8)-O(3)	100.3(5)	O(37)-Mo(9)-O(33)	104.9(4)
O(29)-Mo(7)-O(9)	94.8(4)	O(32)-Mo(8)-O(33)	97.2(4)	O(37)-Mo(9)-O(5)	98.2(4)
O(29)-Mo(7)-O(14)	94.9(3)	O(32)-Mo(8)-O(22)	93.4(4)	O(37)-Mo(9)-O(20)	85.7(3)
O(29)-Mo(7)-O(23)	161.7(3)	O(33)-Mo(8)-O(22)	80.3(3)	O(37)-Mo(9)-O(24)	165.4(3)
O(6)-P(1)-O(4)	107.5(4)	O(6)-P(1)-O(11)	111.2(4)	O(6)-P(1)-O(23)	109.5(4)
O(17)-P(2)-O(22)	111.9(4)	O(17)-P(2)-O(24)	112.2(4)	O(17)-P(2)-O(10)	107.6(4)
O(27)-P(3)-O(25)	112.1(5)	O(27)-P(3)-O(19)	111.3(4)	O(27)-P(3)-O(20)	107.7(4)
O(27)#1-Sr(1)-O(27)	81.9(4)	O(27)#1-Sr(1)-O(22)#1	65.7(2)	O(27)#1-Sr(1)-O(22)	115.3(2)
O(27)#1-Sr(1)-O(4)	118.9(2)	O(27)#1-Sr(1)-O(4)#1	73.1(2)	O(27)#1-Sr(1)-O(6)	170.0(2)
O(27)#1-Sr(1)-O(6)#1	102.3(2)	O(27)#1-Sr(1)-O(3)	58.5(2)	O(39)-Mn(1)-O(25)	171.5(6)
O(39)-Mn(1)-O(30)#2	89.3(6)	O(39)-Mn(1)-O(40)	94.9(6)	O(39)-Mn(1)-O(34)#3	89.8(6)

Symmetry transformations used to generate equivalent atoms: #1 -x,-y,-z; #2 -x+1/2,-y+1/2,-z

Table S2 Selected Hydrogen Bond Lengths () and Bond Angles (°) of complexes 1

D-H...A	d(D-H)	d(H...A)	<D-H...A	d(D...A)	Symmetry
N2-H2...O25	0.86	2.01	161.2	2.840(14)	
O1W-H1WB...O3W	0.85	1.90	105.4	2.28(2)	
O39-H39A...O40	0.85	2.94	93.8	3.117(19)	
O1W-H1WA... O16	0.85	2.94	123.2	3.441(14)	[x, y, z+1]
O1W-H1WB... O34	0.85	2.41	154.8	3.205(13)	[x, -y+3/2, z+1]
O39-H39B...O34	0.85	2.91	93.7	3.080(18)	[x, y, z+1]
O39-H39B...O37	0.85	2.81	122.1	3.339(18)	[-x+1/2, -y+1, z+1/2]
O3W-H3WB...O34	0.85	2.63	120.7	3.147(13)	[x, -y+3/2, z+1]

3. Physical characterization

**Fig. S3** IR spectra of compound 1.

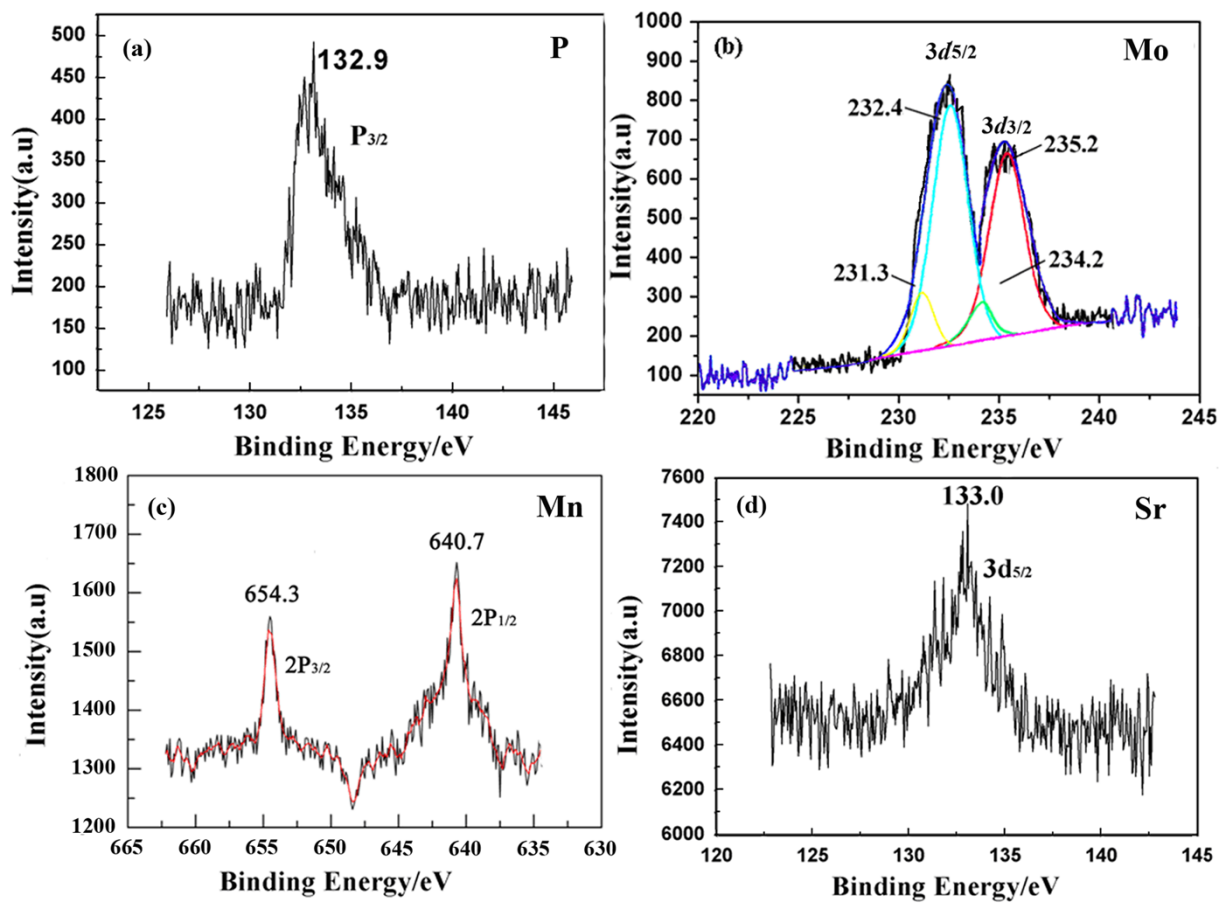


Fig. S4 The XPS spectrum of compound 1 for (a) P, (b) Mo, (c) Mn, and (d) Sr

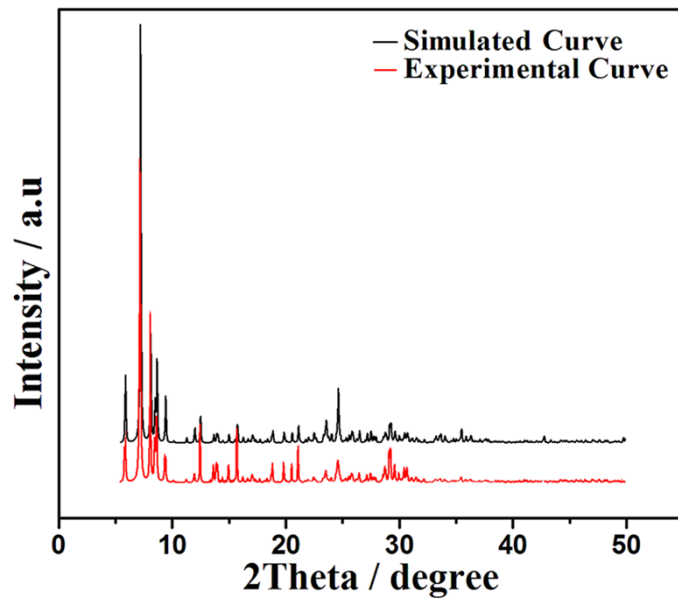


Fig. S5 The PXRD contrast curves of compound 1

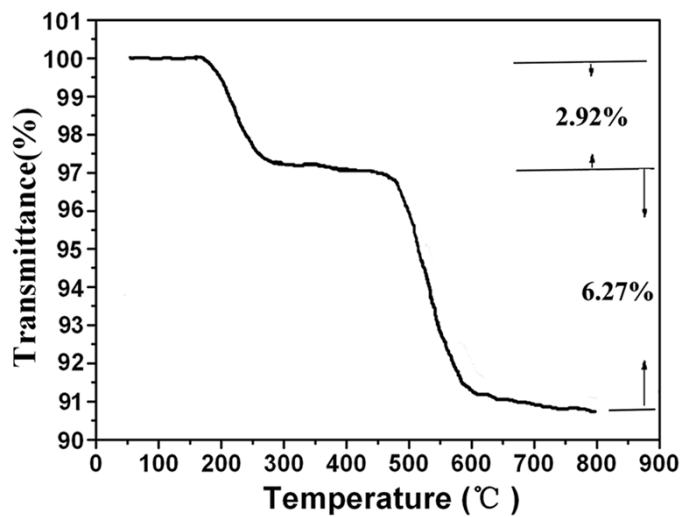


Fig. S6 TG curve of compound 1

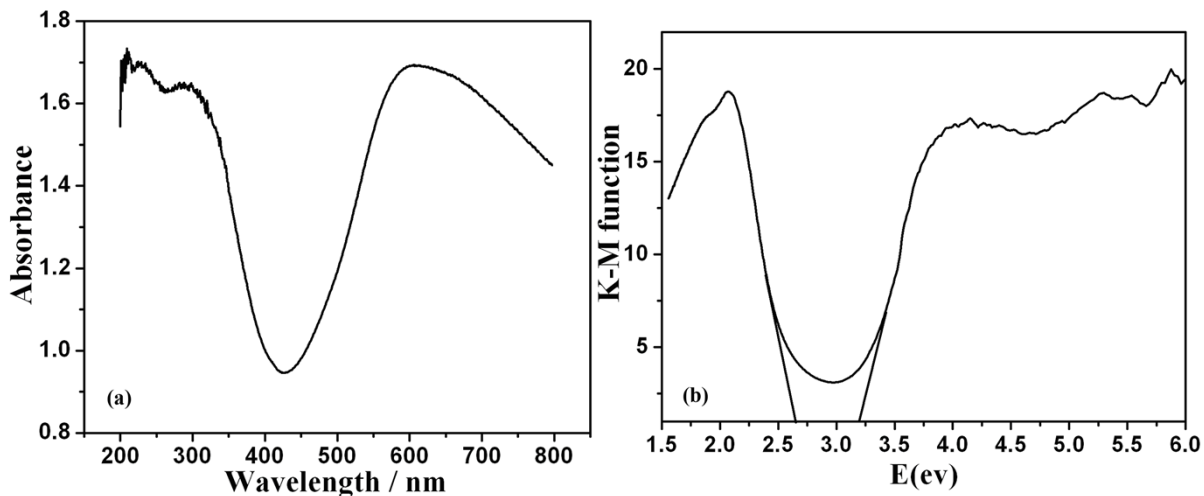


Fig. S7 (a) Solid state UV-vis spectra of catalyst 1; (b) Kubelka-Munk- transformed diffuse reflectance spectra of catalyst 1.

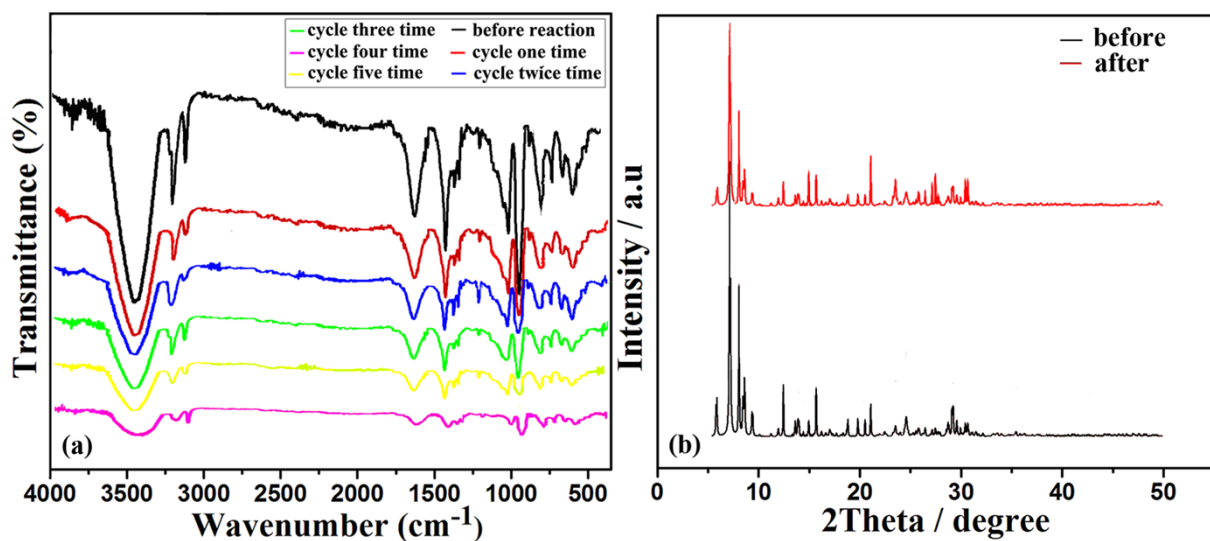


Fig. S8 (a) The IR spectra of catalyst 1 before and after cycle reaction. (b) The XRD patterns of catalyst 1 before and after cycle five time.

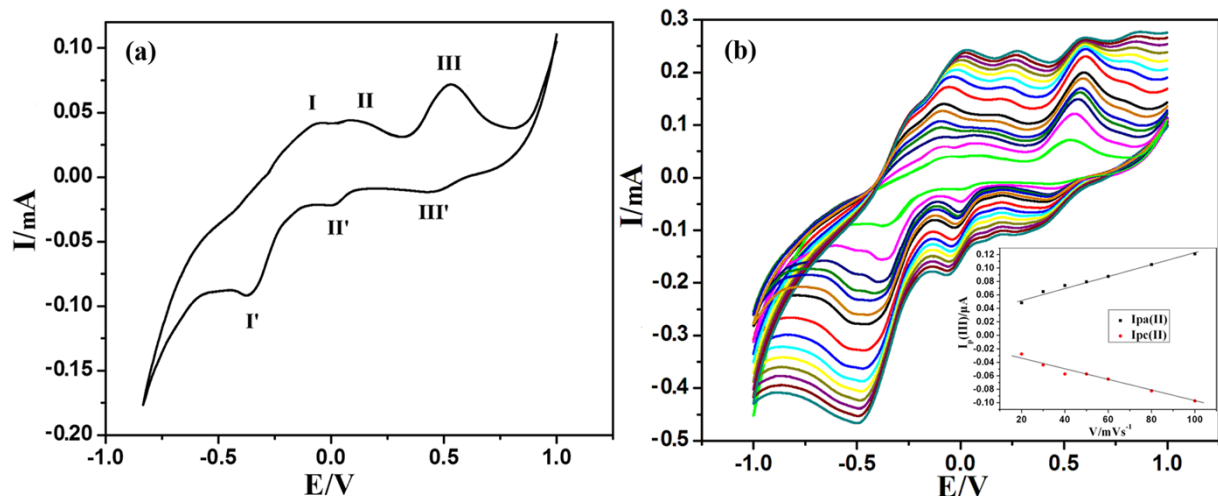


Figure S9 Cyclic voltammograms of (a) 1-CPE at 20 mV s^{-1} and (b) 1-CPE at different scan rate (from inner to outer: 20, 30, 40, 60, 80, 100, 120, 150, 200, 250, 300, 350, 400, 450, 500 mV s^{-1}). Potentials vs. SCE. (Insert plots: The dependence of anodic and cathodic peak II current on scan rates.); The CV of 1-CPE show three reversible redox peaks in the potential range +1.0 to -1.0 V. The mean peak potentials [$E_{1/2} = (E_{pa} + E_{pc})/2$] are +0.46, +0.06, and -0.23 V (based on the CV at 20 mV s^{-1}), which ascribed to three consecutive two-electrom processes of basket $[\text{Sr} \subset \text{P}_6\text{Mo}_{18}\text{O}_{73}]^{8-}$ -heteropolybdate framework. The dependence of anodic and cathodic peak II current on scan rates. At scan rates lower than 100 mV s^{-1} , the peak currents were proportional to the scan rate, indicating that the redox process of the 1-CPE are surface-controlled; while at scan rates higher than 100 mV s^{-1} , the peak currents were proportional to the square root of the scan rate, suggesting that redox process of the 1-CPE is diffusion-controlled.